

Relationship between Orientation of Amorphous Chains and Modulus in Highly Oriented Polypropylene

KENJI YAMADA, MITSUHIRO KAMEZAWA, and MOTOWO TAKAYANAGI, *Department of Applied Chemistry, Faculty of Engineering, Kyushu University, Higashi-ku, Fukuoka 812, Japan*

Synopsis

By using oriented polypropylene prepared by forced quenching in a zone-drawing-type apparatus, the effect of taut tie molecules on the modulus is studied by measuring the changes of superstructure with an increasing draw ratio and the temperature at which the oriented polypropylene was annealed. Superstructure is analyzed by means of an x-ray method, differential scanning calorimetry, thermal shrinkage, birefringence, and infrared spectrum. Modulus increases with an increasing orientation function of amorphous chains, f_a , and is decided only by the value of f_a , so long as the higher value of orientation function of the crystal c axis does not change with the draw ratio or annealing. The taut tie molecules in ultrahigh-modulus polypropylene are loosened by annealing at temperatures below 420 K, but would be incorporated into folded lamellar crystals above the annealing temperature of 420 K. The taut tie molecules does not always have a 3_1 helix conformation.

INTRODUCTION

In our previous work,¹ an ultrahigh-modulus isotactic polypropylene was prepared by forced quenching in a zone-drawing-type apparatus equipped with cooling elements. The maximum value of modulus attained was 15 GPa, which nearly corresponds to half of the crystal modulus along the molecular axis. The zone-drawing method is based on the principle that the necking region is locally heated, which shifts with regulated speed in concert with the propagation of the necking zone on drawing.² In forced quenching, the cooling elements are set close to the heater to effectively remove the annealing effect after zone drawing. The elastic modulus of oriented isotactic polypropylene, prepared in the zone-drawing apparatus, strongly depended on the cooling temperature.¹ When the temperature of the cooling elements is lower than room temperature, a specimen of higher modulus could be obtained. In this article, we tried to clarify the origin of this ultrahigh modulus based on its superstructure.

Filaments of polypropylene of remarkably high modulus and strength have been prepared by Clark and Scott,³ using the two-stage drawing process. The filaments have amorphous regions that are distributed at random within a continuous crystal matrix. Porter, et al.^{4,5} prepared transparent strands of high-density polyethylene of high c -axis orientation by means of a solid-state extrusion in an Instron capillary rheometer and proved that an oriented fringed micelle morphology most nearly represents the ultraoriented structure and the strands contain continuous crystals or crystalline tie chains. According to I. M. Ward, et al.,^{6,7} the sample of ultraoriented polyethylene consists of lamellar stacks of crystallites linked by crystalline bridges. R. G. C. Arridge and P. J. Barham^{8,9} pointed out that in oriented polyethylene after necking, there exists a uniform

distribution of aligned needlelike elements of nearly perfect crystallinity in a less-perfect matrix.

In this work, the superstructure of zone-drawn isotactic polypropylene as a function of the draw ratio is elucidated by measuring the orientation function of crystal *c* axis, birefringence, density, melting behavior, thermal shrinkage, and infrared spectrum. Superstructural change with increasing annealing temperature is also measured for ultrahigh modulus sample through the orientation function of crystal *c* axis, birefringence, density, and infrared spectrum. From the results, the effect of taut tie molecules on modulus is clearer. The thermal stabilities of taut tie molecules are also discussed.

EXPERIMENTAL

Preparation of Sample Used for Zone Drawing

The sample was isotactic polypropylene, MA-8 (Mitsubishi Yuka Co., Ltd.), of which the viscosity-average molecular weight is 510,000. The pellets of MA-8 were compression molded at 493 K in a nitrogen atmosphere to yield a film about 0.5 mm thick, which was rapidly quenched by plunging into ice water. Specimens 1 or 10 mm wide were cut from the quenched films for zone drawing.

The specimens were drawn at drawing speeds of 30–250 mm/min by a tensile tester, Tensilon UTM-III (Toyo Baldwin Co., Ltd.), and an ensemble of the heater, and the cooler was simultaneously shifted at appropriate rate (6.5–16 mm/min) so that the necking region was confined in the heater during drawing. The heater temperature was kept at 410 K, which provided a specimen with the highest modulus.¹ The cooler test temperature was 263 K.

Superstructure Characterization of Zone-Drawn Samples

Modulus

The complex dynamic modulus of zone-drawn sample was measured at room temperature and 3.5 Hz with a viscoelastometer, Rheovibron DDV-III (Toyo Baldwin Co., Ltd.). The complex modulus was taken as the tensile modulus.

X-Ray Measurement

The orientation function of the crystal *c* axis was evaluated from the azimuthal intensity distributions of the (110) and (040) planes by the usual method.

Thermal Behavior

Melting behavior of the zone-drawn sample was measured at a heating rate of 5 K/min by means of a differential scanning calorimeter (DSC), Unix (Rigaku Denki Co., Ltd.). The weight of the sample was approximately 0.5 mg. The heating-rate dependence of the melting temperature was obtained at rates of 1.25 to 80 K/min.

Thermal shrinkage was measured with a Rheovibron DDV-IIB (Toyo Baldwin Co., Ltd.) at a heating rate of about 2 K/min. The thermal shrinkage is scaled by a parameter of $(L_0 - L)/L_0 \times 100$ (%), where L_0 is the original length of the sample at 303 K and L is the value at elevated temperature.

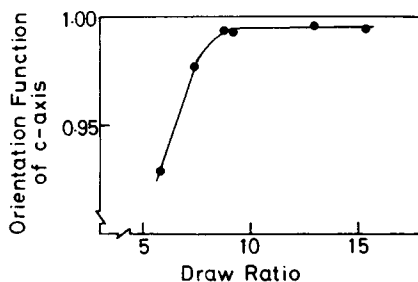


Fig. 1. Increase in orientation function of crystal *c* axis with draw ratio.

Measurements of Birefringence, Density, and Infrared (IR) Spectrum

Birefringence was measured at room temperature with a polarizing microscope, POH (Nippon Kogaku Co., Ltd.). Density was measured at 303 K by a flotation method using a water-ethanol mixture. The IR spectrum was measured at room temperature with a model IR-G (Nippon Bunko Co., Ltd.) spectrometer.

RESULTS

Superstructure Changes in Zone-Drawn Sample with Draw Ratio

Orientation Functions of Crystal C Axis and Amorphous Chains

Figure 1 shows the relationship between orientation function for the crystal *c* axis and the draw ratio. The draw ratio was evaluated from the cross-sectional area reduction. Orientation function of the crystal *c* axis increased rapidly with increasing draw ratio up to draw ratio, $\lambda = 9$, and then leveled off to 0.995 above $\lambda = 9^1$). This tendency is not the experimental limit of the instrument.

Orientation function of amorphous chains, f_a , was evaluated by the following equation:

$$f_a = \frac{\Delta_T - \chi_v f_c \Delta_c^o - \Delta_f}{(1 - \chi_v) \Delta_a^o} \quad (1)$$

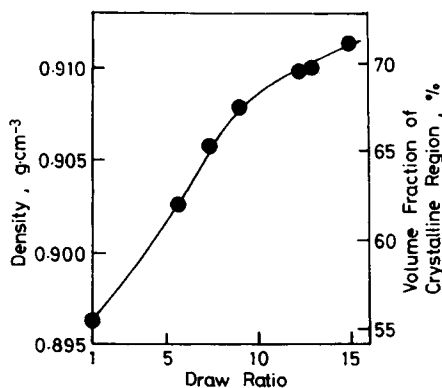


Fig. 2. Increase in density and volume fraction of crystalline region with draw ratio.

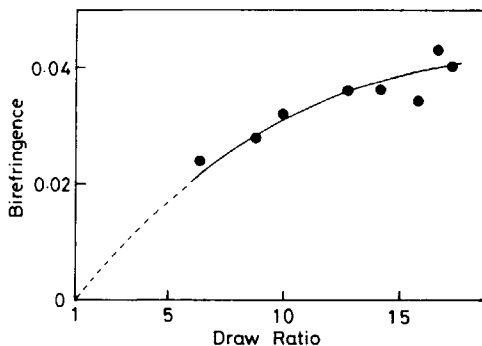


Fig. 3. Increase in birefringence with draw ratio.

where Δ_T is the total birefringence of zone-drawn sample; Δ_a^c and Δ_c^c are the intrinsic birefringences of the crystalline and the amorphous regions, respectively; Δ_f the form birefringence; f_c the orientation function of crystal c axis; and χ_v the volume fraction of crystalline region. The values of Δ_a^c and Δ_c^c for isotactic polypropylene are assumed to be 6.18×10^{-2} and 2.85×10^{-2} , respectively.¹⁰ To evaluate f_a with eq. (1), the values of f_c and χ_v must be measured, even if Δ_f can be neglected. Figure 2 shows variation of the density and volume fraction in the crystalline region, χ_v , as a function of the draw ratio for the samples prepared with the same conditions as Figure 1. The value of χ_v was evaluated by assuming that the densities of crystalline and amorphous regions are 0.933 and 0.853 g/cm²,¹¹ respectively. Density and χ_v increased with increasing draw ratio up to $\lambda \approx 9$, and then its slope decreased above $\lambda \approx 9$. The crystal c -axis orientation leveled off at $\lambda \approx 9$ (Fig. 1). Figure 3 shows variation of birefringence with draw ratio in the same conditions of sample preparation as in Figure 1. Birefringence monotonically increases with draw ratio. Figure 4 shows the orientation function of amorphous chains, f_a evaluated by eq. (1) as a function of λ . The value of Δ_f was neglected in evaluating f_a .¹⁰ The orientation function of amorphous chains increased with λ , but its slope decreased above $\lambda \approx 12$.

Figure 5 shows modulus as a function of λ for the same conditions of sample preparation as in Figure 1. The modulus increased with λ , but the rate decreased above $\lambda \approx 12$ as in Figure 4. Figures 1, 4, and 5 reveal that the modulus depends on orientation functions for the crystal c axis and for the amorphous chains below $\lambda \approx 9$, but only on an orientation function of amorphous chains above $\lambda \approx 9$.

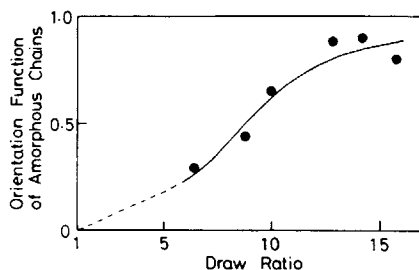


Fig. 4. Increase in orientation function of amorphous chains evaluated by using eq. (1) with draw ratio.

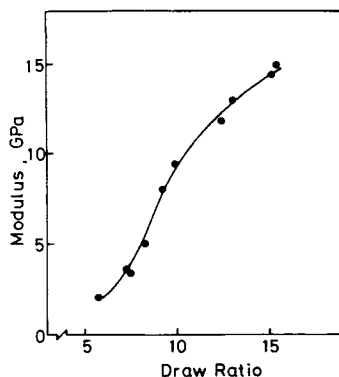


Fig. 5. Increase in modulus with draw ratio.

Changes in Melting Temperature with Draw Ratio and Heating Rate

Figure 6 shows variation of the DSC curves with increasing draw ratio. The main melting peak was shifted to higher temperature with the increasing draw ratio. According to Samuels,¹² this increase is caused by an increase in the amorphous orientation function. This is supported by the results shown in Figures 4 and 6.

Figure 7 shows heating rate dependences of melting temperature for the original and drawn sample of modulus 15 GPa. The final melting on the DSC curve was evaluated as melting temperature. This is only valid if the DSC was also calibrated in this way. The decrease in melting temperature with increasing heating rate, below 10 K/min for both samples, is due to reorganization during heating. Above 10 K/min, the melting temperature of the drawn sample further increased with increasing heating rate—this was ascribed to the so-called superheating phenomenon—in contrast, the original sample scarcely increased.

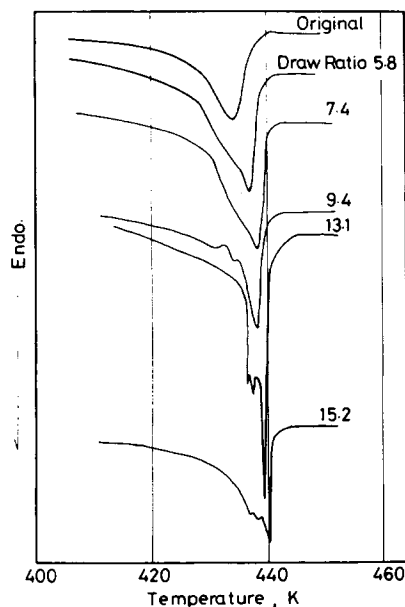


Fig. 6. Variation in DSC curves measured at heating rate of 5 K/min with draw ratio.

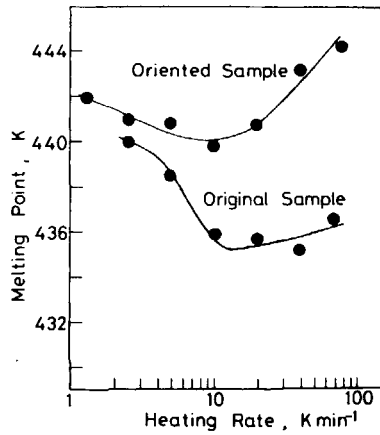


Fig. 7. Variation in melting point with heating rate for original sample and oriented sample with modulus of 15 GPa.

Superstructure Change of Zone-Drawn Sample by Annealing

Changes of Modulus and Orientation Function of Amorphous Chains with Annealing Temperature

Figures 8 and 9 show variations of the birefringence and modulus of the zone-drawn sample with a modulus of 14 GPa, respectively, as a function of annealing temperature, T_a (●). The modulus curve of the sample of modulus 12 GPa, also shown in Figure 9 (○) will be discussed later. The zone-drawn sample

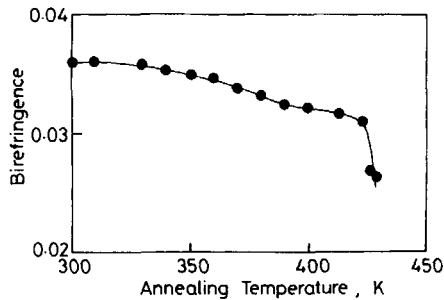


Fig. 8. Decrease in birefringence with annealing temperature for drawn sample of modulus 14 GPa.

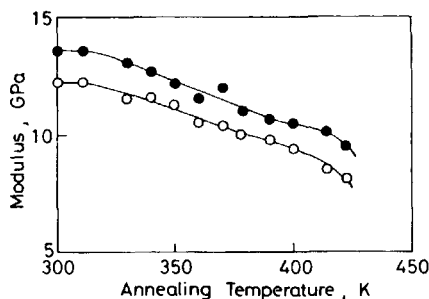


Fig. 9. Decrease in modulus with annealing temperature for drawn samples of moduli of 12 GPa, ○, and 14 GPa, ●.

was annealed for 15 min at each prescribed temperature with free ends, and the birefringence and modulus were then measured at room temperature. Both birefringence and modulus were almost constant up to 310 K, gradually decreasing above that temperature. However, they abruptly decreased in the region 420–430 K. On the other hand, orientation function of the crystal c axis of 0.995 (Fig. 1), scarcely changed up to $T_a = 429$ K. Figure 10 shows variation of density of the same sample (Figs. 8 and 9) as a function of annealing temperature. The density was measured at 303 K (nearly equal to room temperature). Density scarcely changed up to $T_a = 420$ K, but conspicuously increased above that. Figure 11 shows variation in the orientation function of amorphous chains with increasing the annealing temperature. The orientation function of amorphous chains was evaluated by employing eq. (1) and the data in Figures 8 and 10. Both the orientation function of amorphous chains and modulus scarcely changed up to an annealing temperature of 310 K, and gradually decreased from 310 to 420 K. Hence, the modulus depends on the orientation function of amorphous chains.

Figure 12 shows variation of thermal shrinkage with increasing temperature for drawn samples with modulus of 6, 12, and 14 GPa. The thermal shrinkage for the sample with higher modulus was always larger than that with lower modulus over all ranges of temperature. The three curves never intersected.

Changes in IR Spectra with Annealing

The helix bands of isotactic polypropylene are 842, 998, and 1168 cm^{-1} which are associated with 3_1 helix conformation.¹³ These helix bands also depend on crystallinity and nearly disappear in molten state. According to Miyazawa,¹⁴

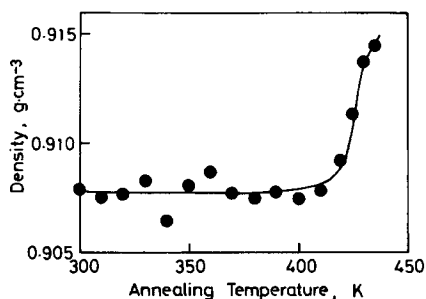


Fig. 10. Increase in density with annealing temperature for drawn sample of modulus of 14 GPa.

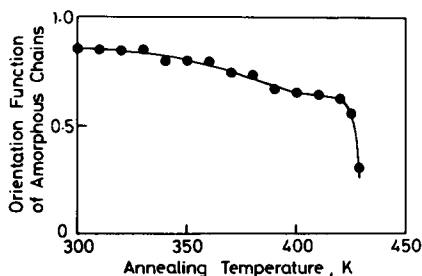


Fig. 11. Decrease in orientation function of amorphous chains evaluated by using eq. (1) with annealing temperature for drawn sample of modulus of 14 GPa.

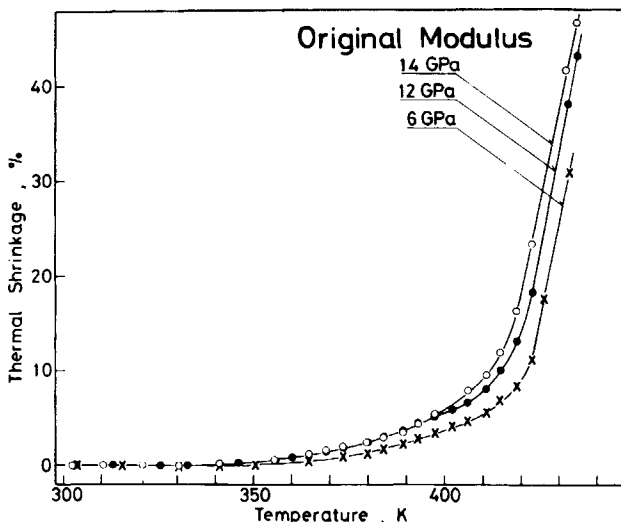


Fig. 12. Increase in thermal shrinkage with temperature for drawn samples of moduli of 6, 12, and 14 GPa.

the band of 842 cm^{-1} is caused by CH_3 rocking and C—C stretching modes, the 998 cm^{-1} band is ascribed to the CH_3 rocking, C—methyl stretching, CH bending, and CH_2 twisting modes, and the 1168 cm^{-1} band to the C—C stretching and CH_3 rocking modes. Figure 13 shows changes of nonpolarized IR spectra with increasing λ . The helix bands abruptly decreased on transformation of the bulk crystallized structure into fiber structure, and slightly decreased after such a transformation which takes place below $\lambda \approx 5$. Since crystallinity, however, increased with λ (Fig. 2), the decrease of absorbance of helix bands may be due to conformational irregularity in the 3_1 helix induced by zone drawing. It is, therefore, inferred that more defects of 3_1 helix conformation are formed in the crystalline region of the oriented sample at higher λ .

Figure 14 shows IR spectra of the samples with modulus of 14 GPa unannealed and annealed for 15 min at 423 and 428 K. On annealing over 430 K, the sample surface became noticeably wavy and the IR spectra could not be measured. IR spectra were virtually unchanged on annealing up to about 423 K, as can be seen in Figure 14. However, comparison of IR spectra at 423 K with the one at 428 K reveals that the absorbance of the helix bands, especially of 842 cm^{-1} slightly increased. The activation energy to convert irregularity of the 3_1 helix conformation to a normal 3_1 helix may be high.

DISCUSSION

Both the modulus and orientation function of amorphous chains in zone-drawn samples always increase with the draw ratio, (Figs. 4 and 5). The orientation function of crystal c axis increased with λ at lower values, but leveled off in the higher λ region (Fig. 1). Therefore, the value of modulus is associated only with orientation function of amorphous chains at high λ . Since in uniaxially oriented samples, modulus appears to be increased by increase of the fraction of taut tie molecules,^{1,15} the increase of orientation function of amorphous chains, f_a , cor-

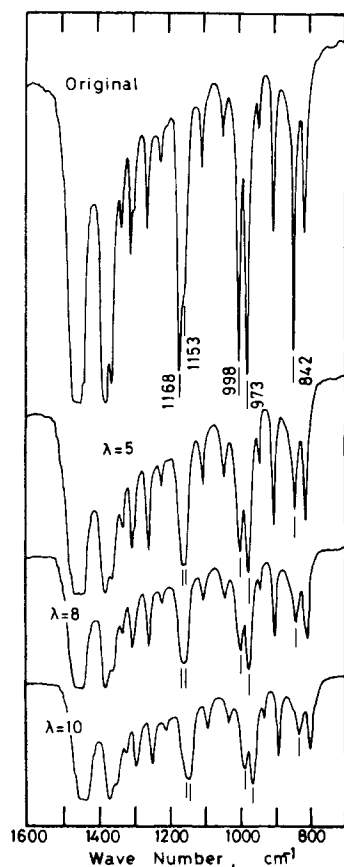


Fig. 13. Variation in IR spectrum with draw ratio.

responds to an increase in the fraction of taut tie molecules in the higher λ region. The increase in the fraction of oriented amorphous chains, viz., taut tie molecules, may contribute to the increase in the density of amorphous region. The probability of aggregating taut tie molecules should increase with the increase in the fraction of taut tie molecules. Such an aggregate of taut tie molecules is similar to a crystal bridge. If the number of taut tie molecules increases, aggregates of extended chains may be formed. This idea is supported by the fact that superheating takes place in the sample with an ultrahigh modulus of 15 GPa: in previous work,¹ the fraction of taut tie molecules in this sample was evaluated as 0.44. According to previous work,¹ the fraction of taut tie molecules, $(1 - \xi)$ will be quantitatively evaluated by the following equation on the basis of the following assumptions: (1) the modulus of taut tie molecules is equal to that of the crystal along the molecular axis; and (2) the modulus of the amorphous phase at room temperature is much less than both the crystal modulus, E_c , of 34 GPa¹⁶ and the modulus of the zone-drawn sample, E , using the composite model composed of the series and parallel connection of crystalline and amorphous regions.

$$(1 - \xi) = E/E_c \quad (2)$$

Figure 15 shows variation of modulus as a function of f_a , being presented by

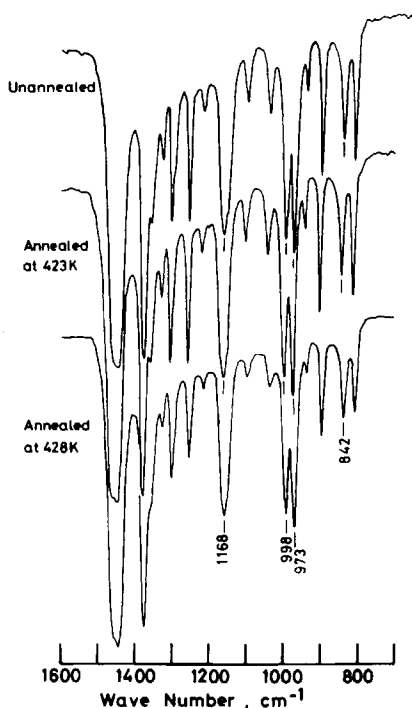


Fig. 14. IR spectra for drawn samples of modulus of 14 GPa unannealed and annealed at 423 and 428 K.

using changes of modulus and f_a as a function of λ or annealing temperature under $f_c = 0.995$. The relationship between modulus and f_a can be represented by a unique curve. Therefore, modulus is decided only by the value of f_a , so long as the higher value of f_c does not change with λ or annealing. When the oriented samples with moduli of 8–15 GPa are annealed, the modulus decreased accompanied with a decrease in orientation function of amorphous chains, f_a (Fig. 15). The decrease in f_a corresponds to loosening of taut tie molecules, which gradually occurs with annealing to 420 K. In the sample of modulus of 14 GPa (Fig. 9), the fraction of taut tie molecules decreases from 0.41 to 0.29 by annealing up to

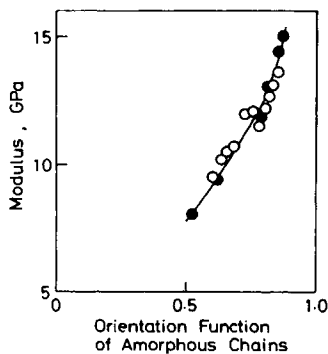


Fig. 15. Increase in modulus with orientation function of amorphous chains under orientation function of crystal c axis of 0.995. Data is presented on basis of changes in modulus and orientation function of amorphous chains as a function of draw ratio, ●, or annealing temperature, ○.

420 K, on the basis of eq. (2). The loosening of tie molecules causes thermal shrinkage (Figs. 11 and 12). The sample with higher modulus always exhibited more thermal shrinkage (Fig. 12). This is reasonable, since the sample of higher modulus would possess the higher fraction of taut tie molecules.

Above 420 K, density conspicuously increased with annealing temperature, whereas both modulus and f_a abruptly decreased (Figs. 9–11). Amorphous chains are incorporated into lamellar crystals by folding themselves, and a major part of these amorphous chains are taut tie molecules. From the result of thermal shrinkage (Fig. 12), more taut tie molecules may be incorporated into folded lamellar crystals above 420 K for the higher modulus sample.

Since the oriented amorphous chains, that is, the taut tie molecules, are gradually loosened with increase of annealing temperature (Fig. 11), the taut tie molecules loosened at lower annealing temperature may be formed in isolated state in amorphous region, whereas those loosened at higher annealing temperature may be done in state, aggregating themselves and therefore become more thermally stable, since the aggregate of taut tie molecules may be more thermally stable. The modulus curves (Fig. 9) never intersected. The fraction of taut tie molecules unloosened at each annealing temperature for the higher modulus sample is always larger than the lower modulus sample and, therefore, the fraction of taut tie molecules with more thermal stability is larger in the higher modulus sample. If there are taut tie molecules with a variety of thermal stabilities, multiple melting peaks would appear in the DSC curve, provided the melting temperature closely depends on f_a . This reasoning is supported by the appearance of multiple melting peaks in the range of the high draw ratio (Fig. 6).

The absorbance of the helix bands hardly changed up to 423 K (Fig. 14). However, f_a continuously decreased with an increase in annealing temperature and thermal shrinkage increased (Figs. 11 and 12). Therefore, the thermal shrinkage of the zone-drawn sample up to 420 K, which may be associated with loosening of taut tie molecules, occurs without converting the irregularity of 3_1 helix conformation to normal 3_1 helix conformation. Furthermore, the conformation of the taut tie molecules and the loosened tie molecules formed by annealing may not be 3_1 helix. Density conspicuously increased above the annealing temperature of 420 K. Absorbance of helix bands is intensified above 428 K (Figs. 10 and 14). Furthermore, the conformation of loosened tie molecules formed by annealing below 420 K may not be 3_1 helix. Hence, the increase of absorbance of helix bands is accompanied by an increase in crystallinity and/or converting irregularity of the 3_1 helix conformation to normal 3_1 helix conformation in the crystalline region.

CONCLUSION

For oriented isotactic polypropylene prepared by forced quenching in a zone-drawing-type apparatus, the increase in modulus at higher draw ratio is caused by the increase in the fraction of taut tie molecules resulting from the increase in orientation of amorphous chains. Further increasing of the draw ratio may cause aggregation of many taut tie molecules in the amorphous region. The taut tie molecules become gradually loosened with increasing annealing temperature above 310 K. The fraction of the taut tie molecules unloosened

by annealing in the sample of higher modulus is always larger than the one of lower modulus at each annealing temperature. The taut tie molecules would be incorporated into lamellar crystals by folding themselves above the annealing temperature of 420 K. Irregularity of 3_1 helix conformation, which would exist in crystalline region as defects, is not restored by annealing at a temperature below 423 K because of the fact that a high-potential barrier exists when transforming irregularity of 3_1 helix conformation into normal 3_1 helix conformation. The conformation of the taut tie molecules and the loosened tie molecules formed by annealing may not be 3_1 helix.

References

1. M. Kamezawa, K. Yamada, and M. Takayanagi, *J. Appl. Polym. Sci.*, **24**, 1227 (1979).
2. H. Kiho and K. Asai, *J. Macromol. Sci., Phys.*, to appear.
3. E. S. Clark and L. S. Scott, *Polym. Eng. Sci.*, **14**, 682 (1974).
4. N. E. Weeks, S. Mori, and R. S. Porter, *J. Polym. Sci. Polym. Phys. Ed.*, **13**, 2031 (1975).
5. N. E. Weeks and R. S. Porter, *J. Polym. Sci. Polym. Phys. Ed.*, **13**, 2049 (1975).
6. J. Clements, R. Jakeways, and I. M. Ward, *Polymer*, **19**, 639 (1978).
7. A. G. Gibson, G. R. Davies, and I. M. Ward, *Polymer*, **19**, 683 (1978).
8. R. G. C. Arridge and P. J. Barham, *J. Polym. Sci. Polym. Phys. Ed.*, **16**, 1297 (1978).
9. R. G. C. Arridge and P. J. Barham, *Polymer*, **19**, 654 (1978).
10. R. J. Samuels, *J. Polym. Sci. Part C*, **20**, 253 (1967).
11. G. Natta, F. Danusso, and G. Moraglio, *Angew. Chem.*, **69**, 686 (1957).
12. R. J. Samuels, *J. Polym. Sci. Polym. Phys. Ed.*, **13**, 1417 (1975).
13. J. P. Luongo, *J. Appl. Polym. Sci.*, **3**, 302 (1960).
14. T. Miyazawa, *J. Polym. Sci. Part C*, **7**, 59 (1964).
15. M. Takayanagi, K. Imada, and T. Kajiyama, *J. Polym. Sci. Part C*, **15**, 75 (1966).
16. I. Sakurada and I. Kaji, *J. Polym. Sci. Part C*, **31**, 57 (1970).

Received January 28, 1980

Accepted July 1, 1980